CHEMICAL ENGINEERING TRANSACTIONS
VOL. 62, 2017
A publication of AIDIC
The Italian Association of Chemical Engineering
Online at www.aidic.it/cet
Guest Editors: Fei Song, Haibo Wang, Fang He

ISBN 978-88-95608- 60-0; **ISSN** 2283-9216
DOI: 10.3303/CET1762111

Study on Fatigue Fracture Mechanism of High Strength TRIP600 Steel for Automobile

Yongli Li, Xiuli Tang

Jilin Institute of Chemical Technology, Jilin 132022, China
YongliLi@126.com

The purpose of this paper was to carry out a series of fatigue tests on a 1.5 mm thick TRIP600MP steel plate. The test data were fitted and the fatigue behaviour was observed by a scanning electron microscope. The test results showed that the fatigue limit of TRIP600 steel plate was 460 MPa under a condition of high cyclic tensile fatigue test with a load frequency of 8 Hz and R=0. The empirical formula of SN curve fitting was lgN=51.1625-16.8574lgσ. The result revealed that the fatigue source of steel plate was mostly under the surface. The principal conclusions were that the extension of the crack was a ductile fracture and the fault zone was brittle fracture.

1. Introduction

TRIP steel was applied to a high-strength automotive steel plate and had characteristics of unique TRIP effect, high work hardening index and strong bake hardening, and thus it became important in manufacturing the automotive production plate (Chapetti et al., 2003). The TRIP effect of the steel maintained a good plasticity. A lot of shapes and complex parts or components were used in the TRIP steel punching indole. The TRIP steel production process in Japan and Germany had accumulated a wealth of technical experiences with the development of different varieties, specifications and performance of the TRIP steel plate (Hilditch et al., 2007). Currently, hot rolling and cold rolling were mainly used to produce good TRIP steel, and the characteristics of the automotive industry and the steel industry have been widely concerned about the prospects for development (Yu and Wang, 2015; Rodríguez-Martínez et al., 2010; Chen et al., 2013; Hu 2016).

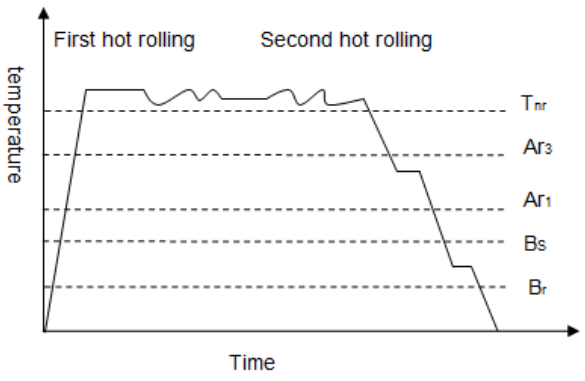

Figure 1: Hot rolling production process of TRIP steel

TRIP steel production process is mainly hot-rolled and cold-rolled as shown in Figure 1. The principle of the hot-rolled TRIP steel production in Figure 1 is employed in the final rolling control after cooling and low temperature curling method. Firstly, the austenite and ferrite two-phase zone is heated to a temperature for a period of time. Then it is slowly cooled to A1 near the steel to retain a certain volume of ferrite. To a certain

Please cite this article as: Yongli Li, Xiuli Tang, 2017, Study on fatigue fracture mechanism of high strength trip600 steel for automobile, Chemical Engineering Transactions, 62, 661-666 DOI:10.3303/CET1762111

volume of the organization, it is quickly cooled to the bainite formation area which began to change the temperature at the coiling, holding temperature and then it is slowly cooled to room temperature. Finally, ferrite-bainite-retained austenite three-phase structure TRIP steel is obtained and the organization conversion is completed.

TRIP steel cold rolling process is shown in Figure 2. The first cold is after the temperature rise to Ah+α two-phase zone of a critical temperature (Ac3~Ac1) annealing. Then in the temperature bainite formation area isothermal quenching, we can get TRIP steel. Strict control of isothermal temperature and isothermal time is an important condition for obtaining stable residual austenite during the cold rolling production of TRIP steel.

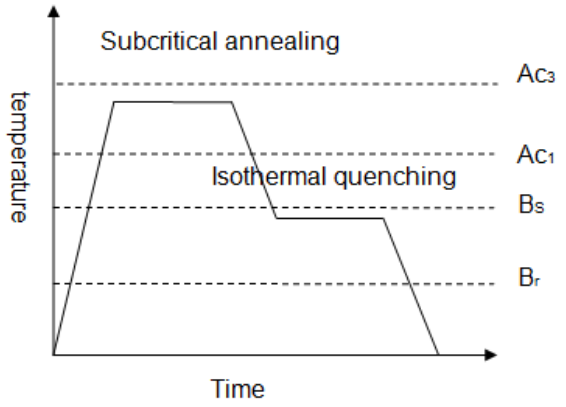

Figure 2: TRIP Steel Technology of Controlled Rolling and Controlled Cold

At present, there were domestic and overseas TRIP steel (Wei and He, 2016). The plated and dynamic mechanical properties of the study were very active. However, the research at home and abroad was mainly focused on the microstructure, heat treatment and other directions. Less research was carried out in terms of the TRIP steel stamping formability, fatigue characteristics, coating properties, welding and so on, which was not conducive to downstream product development applications (Long and Khanna, 2007). Lowering the weight of the car becomes a long-term goal in the automotive industry. Good fatigue performance is necessary for many car bearing structures. TRIP steel, which is a substitute for lightweight steel, must have good fatigue performance before it may have a wider application prospect. However, so far, domestic and overseas research on the fatigue properties of low-carbon silicon-manganese TRIP steel is rarely reported. Therefore, the fatigue performance of TRIP steel with strength of 600MPa is studied in this paper. For the kind of steel, the automotive application for providing theoretical and experimental data was available (Romaniv et al., 1987).

2. Sample preparation and experimental methods

The test material is cold rolled TRIP600 automotive steel plate. Its chemical composition and mechanical properties are shown in Table 1 and Table 2.

Table 1: Chemical composition of TRIP 600MPa steel (wt%)

C	S	P	Mn	Si
0.14	0.008	0.014	1.52	1.24

Table 2: Mechanical properties of TRIP 600MPa steel

σ_s/MPa	σ_b/MPa	δ (%)	n
≥380	≥590	≥23	0.16

Fatigue test was carried out by electromechanical servo fatigue testing machine EHF-UM100 K (SHIMADZU), the maximum test force: dynamic±100 kN, static±150kN. Stress loading error is ±0.5%. Strain measurement error is ±0.5%. Load frequency is 0~50Hz and power supply is 380V. The fracture was analyzed by JSM-5500LV scanning electron microscope (SEM). Since this was a constant amplitude alternating load fatigue test, the shape and size of the specimen are shown in Figure 3.

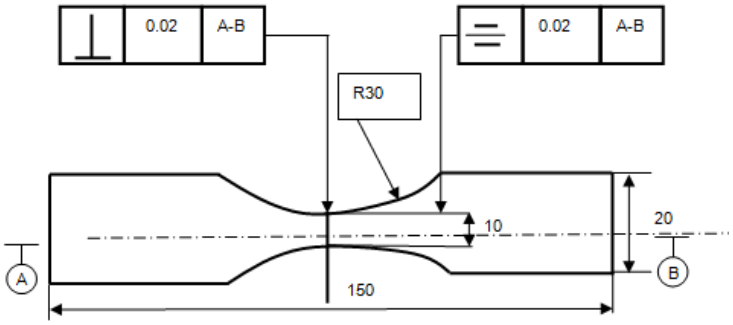

Figure 3: The direction image of fatigue sample

3. Discussion and analysis

3.1 Drawing TRIP600 fatigue S-N curve

The TRIP600 steel plate was loaded with different stress values. Each stress value corresponded to one fatigue cycle. 75% of the TRIP600 tensile curve was the first stress loading value. And the rest of the stress value decreased in turn. The experimental parameters were as follows: (1) load frequency 8Hz; (2) cycle stress ratio; (3) sinusoidal stress loading path. The data for TRIP 600 fatigue performance are shown in Table 3.

Table 3: TRIP600 steel stress fatigue test data

NO.	σ_{max}/MPa	Sectional area /mm^2	Loading force /kN	Cycles
1#	680	18.72	12.7296	29018
2#	660	18.72	12.3552	50342
3#	640	18.72	11.9808	106415
4#	620	18.72	11.606	123102
5#	600	18.72	11.232	131290
6#	580	18.72	10.8576	103689
7#	575	18.72	10.7645	321280
8#	570	18.72	10.6704	525075
9#	565	18.72	10.5768	6375321
10#	560	18.72	10.4832	10000075

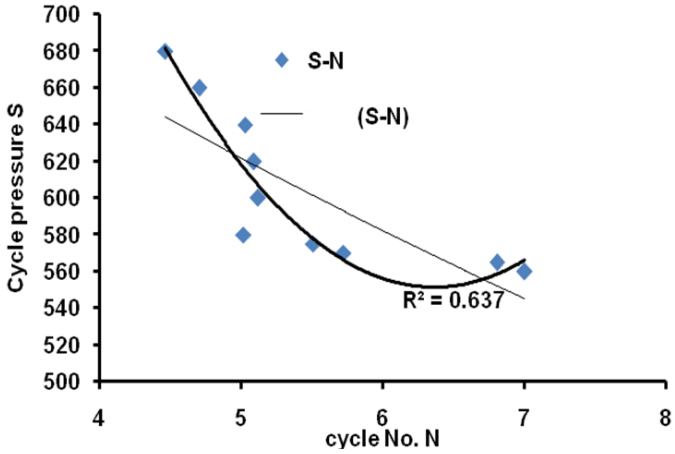

Figure 4: The curve of S-N for TRIP600

According to the experimental data obtained by using the origin software which was employed to draw the S-N curve, the vertical axis, fatigue life of the logarithm X = lgNi for the abscissa to make S-N curve (Figure 4). The fatigue limit of TRIP600 steel plate was 460MPa by single point method. Compared with low carbon steel having the same tensile strength, the fatigue strength of the TRIP600 steel plate was higher and anti-fatigue

performance was better. And the overload fatigue fracture line of TRIP steel was also higher than that of ordinary low carbon steel of 50~60 MPa. (Britainite ferrite+retained austenite) [F+BSUP (BF+AR)], which is mainly due to the multi-phase microstructure of TRIP steel plate. And the TRIP effect of residual austenite phase transition was during fatigue strain. The TRIP effect contributes to improvement of the fatigue properties of high strength steels.

3.2 Fatigue empirical formula fitting analysis

In the car structure and in an anti-fatigue design, a simple and accurate basis should be provided for the TRIP600 steel plate. The left-hand linear equation of S-N curve is fitted by least squares method, which is used as the empirical formula of fatigue of steel plate. The least squares method can be used to determine the best fitting straight line of the fatigue curve. The fitting equation of the least squares method is:

$$\lg N_i = a + b\lg\sigma_i \tag{1}$$

$$a = \frac{1}{n}\sum_{i=1}^{i}\lg N_i - \frac{b}{n}\sum_{i=1}^{i}\lg\sigma_i \tag{2}$$

$$b = \frac{\sum_{i=1}^{n}\lg N_i \lg\sigma_i - \frac{1}{n}\left(\sum_{i=1}^{n}\lg\sigma_i\right)\left(\sum_{i=1}^{n}\lg N_i\right)}{\sum_{i=1}^{n}\left(\lg\sigma_i\right)^2 - \frac{1}{n}\left(\sum_{i=1}^{n}\left(\lg\sigma_i\right)^2\right)} \tag{3}$$

Where lgNi is for the logarithmic average life, n is for the number of data points or stress level series. So the final result of the least squares fitting is:

$$\lg N = 51.1625 - 16.8574\lg\sigma \tag{4}$$

The accurate correlation coefficient of the left line of the S-N curve is

$$r = \frac{L_{SN}}{\sqrt{L_{SS}\bullet L_{NN}}} = 0.7429 \tag{5}$$

r is very close to 1. It can be seen that this fitting equation was reasonable and the error rate was moderate. The formula had certain precision.

$$L_{ss} = \sum_{i=1}^{i}\left(\lg\sigma_i\right)^2 - \frac{1}{n}\left(\sum_{i=1}^{n}\left(\lg\sigma_i\right)^2\right) \tag{6}$$

$$L_{NN} = \sum_{i=1}^{i}\left(\lg N_i\right)^2 - \frac{1}{n}\left(\sum_{i=1}^{n}\left(\lg N_i\right)^2\right) \tag{7}$$

$$L_{SN} = \sum_{i=1}^{i}\lg\sigma_i \lg N_i - \frac{1}{n}\left(\sum_{i=1}^{i}\lg\sigma_i\right)\left(\sum_{i=1}^{i}\lg N_i\right) \tag{8}$$

Computer technology has played an important role in the field of engineering. At the same time we can use the origin software for linear fitting. We will destroy the cycle time N and the stress G into a logarithm (Table 4).

Table 4: Fit the data by Origin

lgσ	2.8325	2.8195	2.8062	2.7792	2.7782	2.7634	2.7558	2.7559
lgN	4.4627	4.7019	5.027	5.093	5.1182	5.0158	5.5076	5.7202

According to the data in Table 4, the fitting result of the S-N curve left branch line is as shown in Figure 5:

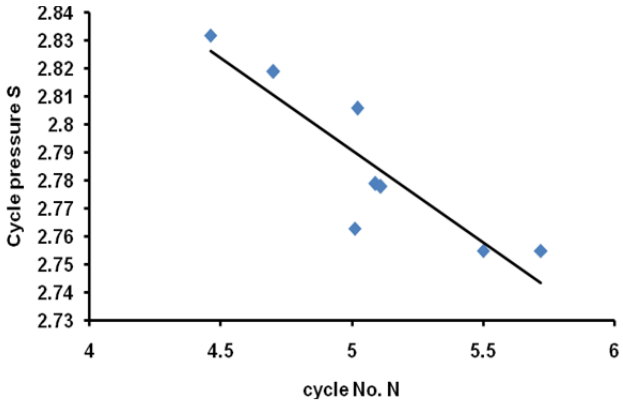

Figure 5: The curve of S-N for TRIP600 in Origin

3.3 Analysis of Constant Strain Fatigue Performance of TRIP600 Steel Plate

The fatigue strength of TRIP600 steel plate was 560 MPa (see the engineering manual). And we found that the specimen was in the pull-pull cycle under the action of longitudinal plastic deformation. This fatigue should be high frequency strain fatigue. TRIP steel fatigue strength was close to the yield strength. It was higher than the yield strength. In order to explore this phenomenon, a high fatigue test on the TRIP600 constant strain was done. The displacement value corresponding to 90% of the selected TRIP600 steel plate was the first load value. The first displacement value measured in the fatigue test was 0.2mm. And the subsequent displacement load value decreased in turn. Experimental parameters: (1) the circulation base of 10 million times; (2) load frequency of 8Hz; (3) cycle strain ratio; (4) stress loading path for the sinusoidal curve. In the process of constant strain fatigue test of TRIP600 steel plate, different displacement values were obtained to obtain the corresponding fatigue life value Nf. Table 5 shows the TRIP600 steel plate constant strain fatigue experimental data.

Table 5: Experimental Data of Constant Stress Fatigue Experiment of TRIP600 Steel Plate

No.	ε_{max}/mm	σ_{max} /mm	N_f/cycles
1#	0.5	521.26	6603
2#	0.45	516.24	13639
3#	0.4	564.85	21333
4#	0.35	536.93	74694
5#	0.325	524.96	88806
6#	0.3	533.63	87170
7#	0.275	520.84	178725
8#	0.25	520.32	573420
9#	0.2	518.7	6764375
10#	0.2	456.35	9859375

3.4 Displacement life curve

The data contained in Tables 4-5 were taken as the ordinate, the logarithmic fatigue life X = lgNi for the abscissa by the origin software is shown in Figure 6.

It can be seen from Figure 5 that the number of cycles was increased as the strain amplitude decreased. When Nf = 1 ×10^7cycles, the TRIP600 steel plate was at the loading frequency of 8Hz, R = 0. It can be seen from the two curves in Figures 4 and 5 that the cyclic stress drops corresponding to the two curves were obviously different when the number of cycles was N = 1 × 10^5. For the curve, in the final stage of cyclic softening, when the number of cycles continued to increase, the magnitude of the stress change was small and was gradually stabilized, and the specimen did not break. After analysis, the TRIP600 steel plate showed overall cyclic hardening. As a result, it broke this process.

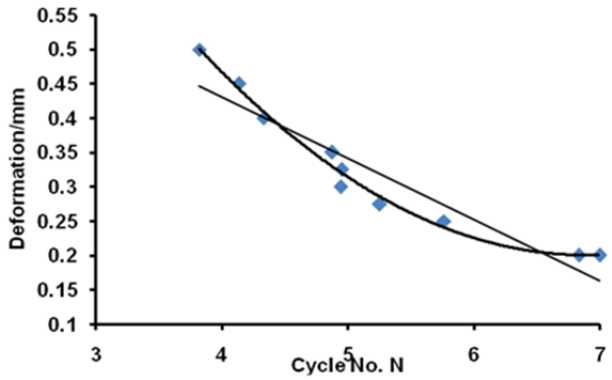

Figure 6: The curve of ε-N for TRIP600

4. Conclusion

Under the action of cyclic load, TRIP600 steel plate showed the characteristics of softening. After the first hardening, the processes of plastic deformation, strengthening and stress reduction and other characteristics of the two steel plates produce high fatigue fracture resistance. From the surface where the stress concentrated, the source where fatigue originated was characterized by ductile fracture in the fatigue crack source. And the extension zone and the transient fault zone werre characterized by brittle fracture. The results showed that the fatigue stress limit of TRIP600 steel plate was 460MPa. And the TRIP steel plate fatigue limit displacement using the fatigue experience of steel plate formula $lgN=51.1625-16.8574lg\sigma$ was 600Mpa.

Acknowledgement

The project supported by the Science and Technology Research Fund of Jilin Institute of Chemical Technology (No. 2017095).

Reference

Chapetti M.D., Tagawa T., Miyata T., 2003, Ultra-long cycle fatigue of high-strength carbon steels part I: review and analysis of the mechanism of failure, Materials Science & Engineering A, 356(1–2), 227-235, DOI: 10.1016/S0921-5093(03)00135-7.

Chen S.W., Jiang M., Zhan Y.R., Huang S. (2013). Formability window of TRIP600 high strength steel sheet at variable blank-holder force, Forging & Stamping Technology, 4, 032.

Hilditch T.B., Speer J.G., Matlock D.K., 2007, Effect of susceptibility to interfacial fracture on fatigue properties of spot-welded high strength sheet steel, Materials & Design, 28(10), 2566-2576, DOI: 10.1016/j.matdes.2006.10.019.

Hu J. (2016). Characterization and modeling of deformation, springback, and failure in advanced high strength steels (AHSSs) (Doctoral dissertation, All Dissertations.

Long X, Khanna S.K., 2007, Fatigue properties and failure characterization of spot welded high strength steel sheet, International Journal of Fatigue, 29(5), 879-886, DOI: 10.1016/j.ijfatigue.2006.08.003.

Rodríguez-Martínez J.A., Pesci R., Rusinek A., Arias A., Zaera R., Pedroche D.A., 2010, Thermo-mechanical behaviour of TRIP 1000 steel sheets subjected to low velocity perforation by conical projectiles at different temperatures, International Journal of Solids and Structures, 47(9), 1268-1284.

Romaniv O.N., Kirillov K.I., Zima Y.V., Nikiforchin G.N., 1987. Relationship of acoustic emission to the kinetics and micromechanism of fatigue failure of high-strength steel with a martensitic structure, Soviet materials science: a transl, of Fiziko-khimicheskaya mekhanika materialov / Academy of Sciences of the Ukrainian SSR, 23(2), 156-160, DOI: 10.1007/BF00718136.

Wei K., He B.L., 2016, Failure Mechanism of Very High Cycle Fatigue for High Strength Steels, Key Engineering Materials, 664, 275-281, DOI: 10.4028/www.scientific.net/KEM.664.275.

Yu H., Wang Y., 2015, Fracture performance of high strength steels, aluminium and magnesium alloys during plastic deformation, In MATEC Web of Conferences, 21, 07001, DOI: 10.1051/matecconf/20152107001.